J. Appl. Comput. Mech., 6(4) (2020) 878-892
DOI: 10.22055/JACM.2019.14847

ISSN: 2383-4536
jacm.scu.ac.ir

M&MoCS

Shahid Chamran University of Ahvaz

Journal of Applied and Computational Mechanics

Research Paper

Stress Intensity Factor Expression for Welded Butt Joint with Undercut and Inclined Lack of Penetration Defects considering the Effect of Joint Shape

Akbar Jafari[1], Mohsen Rezaeian Akbarzadeh[2]

[1] Department of Mechanical Engineering, Amirkabir University of Technology, Tehran, Iran, Email: aj68@aut.ac.ir

[2] Department of Mechanical Engineering, Amirkabir University of Technology, Tehran, Iran, Email: rezaeian@aut.ac.ir

Received July 14 2019; Revised September 17 2019; Accepted for publication October 17 2019.
Corresponding author: A. Jafari (aj68@aut.ac.ir)

Abstract. In this paper, the stress intensity factor (SIF) expression for defected butt welds containing undercut and inclined lack of penetration (LOP) subject to far-field tensile stress is derived. Some of the standards such as ISO 5817 and BS EN 25817 have specified allowable limits for the length of the undercut and LOP defects and for the height of the weld. In addition, EN 29692 standard has determined an acceptable range for the groove angle. In this paper, the effect of these acceptable geometries on stress intensity factor (SIF) of butt welded joint is investigated through following steps: i) elastic analyses to predict crack tip stress intensity (K_I, K_{II}) and shape factors, ii) approximation of shape factors by Response Surface Method (RSM). These expressions provide design guidelines for welded butt joint containing unavoidable undercut and inclined lack of penetration (LOP) defects.

Keywords: Stress intensity factor; Butt welded joint; Undercut; Lack of penetration; Response surface method.

1. Introduction

Improved welding processes have been developed and used for decades in industrial applications. Defects introduced in economic welded joints are unavoidable. For this reason, most of the welded joints have crack-like defects such as, lack of penetration (LOP) at the weld root, undercut at the weld toes, slag inclusions, and gas pores. These defects have important impacts on the load carrying behavior of the joints. Due to the weld reinforcement, the stress concentration at the weld toe and defect location is usually too high [1]. The LOP defect during the welding process comes from some difficulties in the weld root access and can be considered as the initial crack that may significantly affect the fatigue life and static behavior of the joint [2]. The undercut defects can be divided into the three types, i.e. wide and curved, narrow and very narrow (crack-like), and shallow and narrow (micro-flaw with depth up to about 0.25 mm [1]. In this study, LOP and undercut defects are considered as initial cracks in separate studies.

In order to prevent the formation of the defects, it is necessary to know the physical and mechanical properties of the materials and to make a suitable choice of the electrodes, joint design, fit-up, and welding parameters [3]. Aidy et al. [4] showed that welding process also plays an important role in the defects formation, in a way that in more expensive processes such as Tungsten Inert Gas (TIG) welding, observed LOP, undercut and internal porosity defects are less likely compared to economical Metal Inert Gas (MIG) and Manual Metal Arc (MMA) processes.

Most of the structural steels, operating below critical temperatures, show a transition from the ductile to the brittle behavior. Brittle fracture can even occur at normal operating temperatures above critical point in a steel structure which has notches or crack-like defects [5-7].

Published online: October 20 2020

Weld design can be conducted based on traditional and/or modern methods. Although traditional methods are still used widely but the modern technique of reliability based design have received noticeable attention [8, 9]. To assess the safety and reliability of cracked welded joints, probabilistic fracture mechanic theory might be used so as to provide true and creditable assessment by properly considering loads, geometry, and material parameters as random variables [10]. The well-known Finite Element (FE) method could precisely analyze local stress details of a structure [11] and hence the combination of this method with reliability based technique results in safer and more reliable joints.

It is well known that weld reinforcement is usually ignored in the SIF calculation. However, it's shape parameter may have some significant effects on SIF. Hobbacher [12] calculated stress intensity factors "SIF" for a variety of welded joints such as non-load carrying transverse and longitudinal attachments, cruciform joints with K-butt and with fillet welds, and lap joints with fillet welds. Stress intensity factor for cracks at the weld toe or root of fillet welded joints is obtained by Frank et al. [13]. In this work, the results of the FE analysis showed that the SIF was a function of weld size, weld angle, plate thickness and weld penetration and, some expressions to estimate the stress intensity factor were developed. Discontinuous shape factor expressions for a variety of welded joints are indicated in [14] which aren't suitable for structural reliability assessments. Effects of the profile and geometry of butt welds having crack-like defects, such as undercut or inclined LOP, on the SIF have not yet been sufficiently investigated. Wang et al. [9, 15] developed a "mode I" SIF expression for the butt welded joint containing center and single-edge crack in weld metal regarding joint shape and effect of weld reinforcement.

The purpose of the present study is to obtain a more accurate expression for SIF of defected butt welded joint because of undercut and inclined LOP subject to far-field tensile stress. In this study, four independent, dimensionless parameters of weld geometry namely, ratios of the weld width, weld height, weld toe radius, and crack length to base metal thickness were considered. Based on ISO 5817 [16], BS EN 25817 [17] and EN 29692 [18] standards, some allowable values for the length of the undercut and LOP defects, and also weld size and groove angle are recommended. However, these might have unknown impact on their SIF subject to investigate. Hence the body of present study comprises two parts: i) elastic analyses to predict shape factors and crack tip SIF (K_I, K_{II}), ii) approximation of shape factor by RSM, both with some expressions to provide design tools for the butt joints containing undercut and LOP defects.

2. Linear Elastic Fracture Mechanics

The stress intensity factor K in the three fracture modes namely I, II and III is generally defined by the following function:

$$K = Y\sigma\sqrt{\pi a} \tag{1}$$

where, σ, a and Y are stress, crack length, and shape factor, respectively. Because of lack of an appropriate expression for shape factor, reinforcement has rarely been considered in the SIF calculations [19, 20]. Weld reinforcement may endanger the joint due to the stress concentration caused at the weld toe. Kirkhope et al. [21, 22] and Nguyen & Wahab [23] concluded that welded joint fatigue properties can be improved by weld toe smooth transition. Fig. 1 shows a schematic diagram of butt welded joint with an undercut as a sharp tip notch treated as a crack. The indicated parameters in this figure are as follows: w weld width, h weld height, r weld toe transition radius, a_u undercut defect length, a_l LOP defect length, and t base metal thickness. Another important parameter effecting stress concentration at the toe area is weld toe angle, which is considered in this study indirectly by weld geometry as its value is a function of w h, and r. The shaded area represents the weld fillet. Dimension r could be obtained by machining or some other means. The LOP defect could lead in sharp tips between weld metal and base metal acting as a dangerous real crack, as noted at zone A in Fig.1 and in X-shaped bevels would mostly be oblique and not perpendicular to the longitudinal stress. Therefore, the crack tip stress will be a combination of tension and shear that results in a mixed fracture mode I and II as is also called plane mixed mode [24].

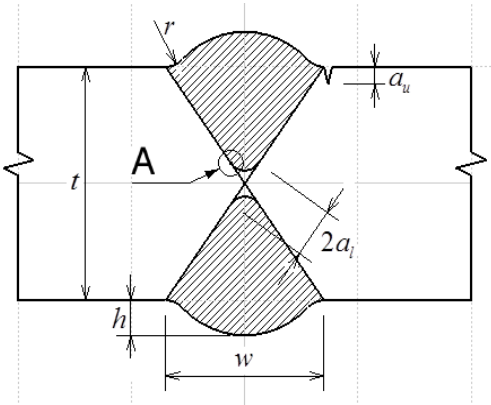

Fig. 1. Geometry of modified butt joint with inclined LOP and undercut defect, under longitudinal load.

3. The Stress Intensity Factor

As introduced, the weld LOP and undercut defects could be modeled as real cracks. Residual stress is not considered in the SIF calculation, however, it can be treated as an extra stress in estimation of the SIF. The investigation was performed on four independent geometric parameters namely, the weld width, height, toe radius, and crack length dimensiolessly in their ratios to base metal thickness for generalization. In order to study the effect of these parameters on the SIF in eq. (1), their impact on the shape factor should be determined and, the following steps are performed: (1) calculation of K_I and K_{II} using FE analyses, (2) Calculation of the shape factor in all the analyses, using eqs. (2) and (3).

$$Y_I = \frac{K_I}{\sigma\sqrt{\pi a}} \tag{2}$$

$$Y_{II} = \frac{K_{II}}{\sigma\sqrt{\pi a}} \tag{3}$$

and (3) Obtaining the correlation between shape factor with the crack and weld geometrical parameters for both inclined LOP and undercut defects using RSM. In the experimental design of RSM for complex systems with many parameters, first a screening experiment is carried out in order to identify important parameters and then, subsequent experiments are designed for more precision [25].

3.1 Finite element method

In this study, the weld reinforcement curve is defined by three successive arcs. One of the arcs is for weld reinforcement body and the other two with the same radius for smooth toe transitions at both sides. Assuming plane strain condition, two-dimensional FE model was applied. In order to obtain accurate results, meshes next to the crack tip were made finely (with a ratio of 0.002 for minimum mesh size) and gradually enlarged, for farther points from the crack tip. An isotropic and homogeneous material under a moderate stress is used in the FEM analysis. The SIFs are calculated via displacement extrapolation method and nodal displacements of elements around the crack tip to obtain crack tip singular stresses [26-29].

To validate the FE solutions for SIF, a limited number of analyses were performed initially for some cases as is reported in the literature. Thus, some validations against the experiments and FEM analyses reportedby Wang et al. [15] were performed. In [15], a center cracked perpendicular to the axial stress for the butt welded joint, based on four independent parameters, i.e. width, height, and toe radius of the weld, and crack length in the fracture mode I were studied. In their FEM, K_I is obtained through J-integral method and then, eq. (2) is used for corresponding shape factor calculation.

From eq.(2), shape factor Y_I can be obtained using the following equation:

$$Y_I = \frac{K_{IC}}{\sigma_C\sqrt{\pi a}} \tag{4}$$

So, the shape factor Y_I of experimental result can be obtained by substituting the fracture toughness K_{IC} of weld metal, critical tensile stress σ_C, and initial crack length a into eq. (4). Wang et al. [15] tested three types of center-cracked butt joints by utilizing the material testing machine (CSS-44300). In all these experiments, fracture toughness, K_{IC}, of weld metal was 34.8 MPa $(m)^{½}$ and the base metal thickness, t, was 10 mm. All of these center cracks were made artificially with the same lengths, i.e. a=2mm.

The results of the present study comparable with the results of Wang et al.'s experiments and models are given in Table 1. The comparison of these results for all of the three types of butt joints show only small discrepancies and justifies the accuracy of the present SIF calculations .

Table 1. Comparison of the results of present study with that of Wang's experiments and simulations.

#	h (mm)	$w/2$ (mm)	r (mm)	σ_C (MPa)	Y (shape factor)			Discrepancies (%) (With respect to experiment)	
					Experiment (Wang et al)	Simulation (Wang et al)	Simulation (present study)	Simulation (Wang et al)	Simulation (Present study)
1	1.5	6.5	0	456	0.96238	0.91848	0.95199	4.78	1.09
2	1.5	15	12	498	0.88121	0.84742	0.84897	3.99	3.80
3	2.5	15	12	550	0.79789	0.77942	0.76101	2.37	4.85

Compared with the present study, more precision of Wang's no 2 and 3 experiments use is made of weld fillet width exceeding what the standards recommend which are not practical. However confined to the generally accepted fillet section geometries, one could confirm the better predictions that go with the present simulations.

Equation (5) is a variant of what proposed in [15].

$$Y_I = \left\{1 + s_1 \frac{2D}{2D+1} \exp\left[-\frac{\frac{B}{2D+1} - \frac{8DBC}{(B^2+4D^2)(2D+1)}}{4s_2D^2 + 2s_3D + s_4}\right]\right\} \times \frac{1}{\sqrt{(1+2D)^2 - A^2}} \quad (5)$$

where crack and weld parameters A, B, C, and D are a/t, w/t, r/t, and h/t ratios, respectively. In addition, constants s_1, s_2, s_3, and s_4 are 1.77633, -0.49536, 0.66789 and 0.75115, respectively.

Availability of a closed-form differentiable expression for the failure state function in a rather simpler form than eq. (5) is essential for application of first/second order reliability techniques (i.e. FORM/SORM) to estimate reliability index [30]. Employing the RSM for a specific region of variables is one of the recommended approaches to provide requirements of application of these advanced probabilistic techniques.

3.2 The SIF expression for welded joint containing inclined LOP defects

ISO 5817 [16] and BS EN 25817 [17] standards have specified some allowable ranges for the length of LOP and weld height as shown in Table 2. The LOP lengths listed in this table are taken $2a_l$. In addition, EN 29692 [18] standard has determined an allowable range for the groove angle (α), which is given in Table 3.

Table 2. Acceptable ranges of the length of LOP and weld height for standard quality levels.

Standard	Thickness (mm)	Limits for lack of penetration for quality levels		
		D	C	B
Acceptable ranges of the length of LOP for quality levels.				
ISO5817 [16]	>0.5	<0.2t (max 2mm)	<0.1t (max 1.5mm)	Not permitted
BS EN 25817 [17]	-			
Acceptable ranges of the weld height for quality levels.				
ISO5817 [16]	>0.5	h ≤ 1mm+0.25w (max 10mm)	h ≤ 1mm+0.15w (max 7mm)	h ≤ 1mm+0.1w (max 5mm)
BS EN 25817 [17]	-			

Table 3. Allowable ranges of the groove angle based on EN 29692 standard [18].

Illustration and cross section	Thickness (mm)	Angle α	b
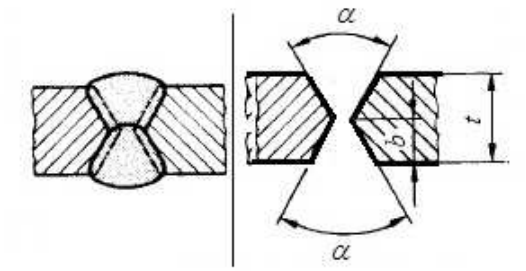	$t > 10$	$40^\circ \le \alpha \le 60^\circ$	$b = \frac{t}{2}$

This study was focused on the allowable limits and r/t ratio considered to range from 0 to 1. All the resultant Y_I, Y_{II} expressions would cover these ranges. A quarter of the FE model is established due to the geometric and loading symmetry of the joint. The joint shown in Fig. 2 has a thickness (t) of 10 mm and w/t=0.7, h/t=0.15, r/t=0.1, a_l/t=0.1. Decision made for ranges of factor levels in multi-level factorial design is based on parameter's significance and their F-values as resulted in the screening experiments of 2-level factorial design.

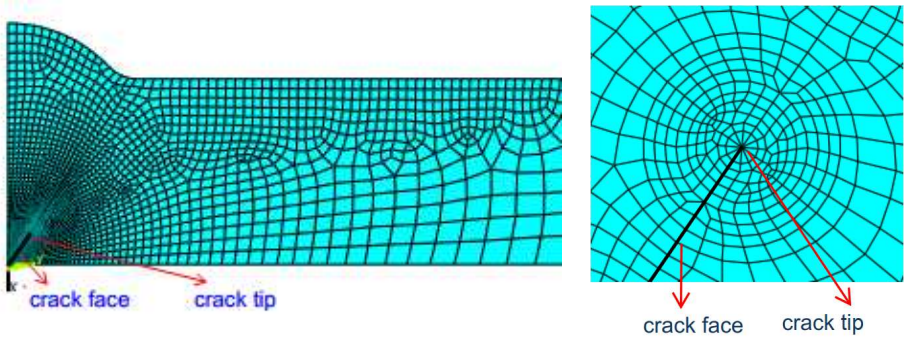

(a) (b)

Fig. 2. (1) FE model of 1/4 butt welded joint with LOP and (2) FE model of meshes near the crack tip.

3.2.1 Two-level factorial design for LOP defect

Lower and higher levels of the parameters shown in Table 4 were used to obtain expressions for Y_I and Y_{II} by RSM with 2-level full factorial design. The design matrix and the responses are shown in Table 5.

Table 4. Factor levels for the 2-level factorial design in the LOP study.

Factors	Low level (-1)	High level (+1)
$A=a_l/t$	0.05	0.1
$B=w/t$	0.35	0.7
$C=r/t$	0.05	0.1
$D=h/t$	0.075	0.15

Table 5. The 2-level factorial design Matrix and responses for the LOP study.

Run	Factor Levels				Responses	
	A	*B*	*C*	*D*	Y_I	Y_{II}
1	-1	1	1	-1	0.5506	0.3840
2	1	-1	1	1	0.7375	0.1803
3	-1	-1	-1	1	0.7238	0.1756
4	-1	1	-1	-1	0.5496	0.3840
5	1	1	-1	1	0.5480	0.4012
6	1	-1	1	-1	0.7376	0.1798
7	-1	1	-1	1	0.5425	0.3941
8	1	1	-1	-1	0.5561	0.3908
9	1	-1	-1	-1	0.7374	0.1810
10	1	1	1	1	0.5508	0.4002
11	1	1	1	-1	0.5572	0.3910
12	-1	-1	1	1	0.7238	0.1746
13	-1	1	1	1	0.5451	0.3931
14	1	-1	-1	1	0.7372	0.1811
15	-1	-1	-1	-1	0.7239	0.1755
16	-1	-1	1	-1	0.7242	0.1743

Each combination of factor levels provides a treatment in formal statistical analysis of data in order to find multi factor effects and their interactions. In this technique use is made of analysis of variances (ANOVA), where parameter P is an indication of probability of no factor effect and parameter F as the relevant critical value of F-test is the ratio of mean square variations of response attributable to a factor to the mean square of standard error. These two parameters could validate a factor effect based on statistical inference singly or mutually [25].

Table 6. The F-value, P-value and coefficient of Y_I equation terms in the LOP study.

Term	Coef.	F value	P value
Intercept	0.64	-	-
A	4.9e-3	40169.3	0.0032
B	-0.090	1.38E+7	0.0002
C	5.3e-4	472.9	0.0293
D	-1.7e-3	5122.8	0.0089
AB	-1.9e-3	5893.4	0.0083
AC	1.2e-5	0.3	0.6989
AD	-1.0e-4	18.5	0.1453
BC	4.2e-4	297.7	0.0369
BD	-1.6e3	4512.0	0.0095
CD	1.8e-4	55.4	0.0850
ABC	5.8e-6	0.058	0.8492
ABD	-1.1e-4	22.7	0.1317
ACD	4.8e-5	2.9	0.3394
BCD	2.2e-4	81.9	0.0701

Table 7. The F-value, P-value and coefficient of Y_{II} equation terms in the LOP study.

Term	Coef.	F value	P value
Intercept	0.29	-	-
A	3.1e-3	20247.6	0.0045
B	0.11	2.38e+7	0.0001
C	-3.9e-4	307.5	0.0363
D	2.5e-3	12801.0	0.0056
AB	3.6e-4	265.1	0.0390
AC	1.1e-5	0.25	0.7048
AD	3.7e-5	2.83	0.3413
BC	1.5e-4	48.6	0.0907
BD	2.4e-3	11607.5	0.0059
CD	-1.0e-4	24.6	0.1266
ABC	-9.4e-6	0.18	0.7422
ABD	8.4e-6	0.14	0.7691
ACD	1.2e-5	0.28	0.6923
BCD	-1.7e-4	60.61	0.0813

Table 8. Goodness-of-Fit indices for obtained Y_I and Y_{II} equations in the LOP study.

Index	Y_I	Y_{II}
R^2	1.0000	1.0000
adjusted_ R^2	0.9999	1.0000
Pred_R^2	0.9999	1.0000
Adeq. precision	414.02	661.38

The values of F and P together with the response coefficients for coded factors are shown in Tables 6 and 7. The magnitude of coefficients could particularly be used for comparing relative importance of factors. Effects with lower F-value and higher P-value could be of no importance and are removed from the model noting the condition that the results of Goodness-of-Fit indices as shown in Table 8 are satisfactory.

As shown in Tables 6 and 7, the weld width factor B: w/t has the greatest impact on both shape factors. Then, factor A: a_l/t and factor D: h/t have a great effect on the responses Y_I and Y_{II}, respectively. The r/t ratio in expressions for Y_I and Y_{II} may be removed because of very low effect on both responses. Equations 6 and 7 are obtained for shape factors Y_I and Y_{II}., respectively. Goodness of fit indices, including, R^2, adjusted_R^2, Pred_R^2 and adequate precision are given in Table 8 where, the adequate factor effect is justified.

In both of the proposed models, adequacy of indices as all are near to 1, indicate a high goodness of fit and are justified.

$$Y_I = 0.869+0.420A-0.456B+0.021C+0.084D-0.427AB-0.249BD \tag{6}$$

$$Y_{II} = -0.031+0.125A+0.572B-0.015C-0.123D+0.361BD \tag{7}$$

Table 9. Factor levels for the multi-level full factorial design in the LOP study.

Factors	levels			
	1	2	3	4
$A=a_l/t$	0.033	0.066	0.1	
$B=w/t$	0.35	0.45	0.55	0.70
$C=r/t$	0.05	0.1		
$D=h/t$	0.075	0.15		

Table 10. Factor levels for the multi-level full factorial design in the LOP study.

Run	Factor Levels				Responses	
	A	B	C	D	Y_I	Y_{II}
1	1	1	1	1	0.7214	0.1744
2	3	4	2	2	0.5508	0.4002
3	3	1	2	1	0.7376	0.1798
4	2	2	1	1	0.6881	0.2550
5	2	1	2	2	0.7274	0.1762
6	3	2	1	1	0.6966	0.2602
7	3	3	2	2	0.6443	0.3272
8	3	3	2	1	0.6453	0.3236
9	2	4	1	2	0.5439	0.3959
10	1	2	2	2	0.6840	0.2518
11	3	4	2	1	0.5571	0.3910
12	3	2	1	2	0.6964	0.2620
13	2	2	2	1	0.6889	0.2540
14	1	2	1	1	0.6832	0.2520
15	3	1	1	1	0.7374	0.1810
16	1	3	2	1	0.6345	0.3148
17	2	2	2	2	0.6890	0.2548
18	1	3	2	2	0.6338	0.3183
19	1	1	2	1	0.7218	0.1733
20	2	1	2	1	0.7275	0.1757
21	1	3	1	2	0.6320	0.3204
22	2	1	1	1	0.7271	0.1768
23	3	2	2	1	0.6975	0.2592
24	2	3	1	2	0.6358	0.3237
25	2	2	1	2	0.6880	0.2568
26	1	2	1	2	0.6832	0.2537
27	3	2	2	2	0.6975	0.2599
28	2	4	1	1	0.5513	0.3855
29	1	1	2	2	0.7215	0.1738
30	1	4	2	2	0.5440	0.3920
31	1	4	1	2	0.5412	0.3931
32	2	3	2	1	0.6384	0.3180
33	3	4	1	1	0.5561	0.3908
34	1	4	2	1	0.5495	0.3827
35	1	2	2	1	0.6841	0.2509
36	3	3	1	1	0.6441	0.3242
37	2	4	2	2	0.5467	0.3947
38	2	3	2	2	0.6376	0.3216
39	2	1	1	2	0.7271	0.1770
40	3	4	1	2	0.5480	0.4012
41	3	1	1	2	0.7372	0.1811
42	1	3	1	1	0.6333	0.3154
43	3	1	2	2	0.7375	0.1803
44	1	4	1	1	0.5483	0.3827
45	3	3	1	2	0.6423	0.3293
46	1	1	1	2	0.7213	0.1745
47	2	3	1	1	0.6372	0.3186
48	2	4	2	1	0.5524	0.3856

3.2.2 Multi-level full factorial design

Referred to significance of factors as presented in Tables 6 and 7, a number of levels were added for important parameters in order to estimate curvature of the response surface. Parameter levels for multi-level full factorial design are shown in Table 9 and the design matrix and the responses are shown in Table 10. The F-value, P-value and resulted factor coefficients for Y expressions are given in Tables 11 and 12.

Table 11. The F-value, P-value and factor coefficients for Y_I expression in the LOP study.

Term	Coef.	F value	P value
Intercept	0.65	-	-
A	5.7e-3	29176.8	<0.0001
B	-0.094	8.63e+5	<0.0001
C	6.9e-4	362.1	<0.0001
D	-3.7e-4	101.6	<0.0001
AB	-2.2e-3	5932.2	<0.0001
AC	2.0e-5	0.89	0.3537
AD	-1.0e-4	22.64	<0.0001
BC	4.1e-4	314.85	<0.0001
BD	-1.6e-3	4841.0	<0.0001
CD	1.6e-4	83.0	<0.0001
A^2	1.4e-3	1581.9	<0.0001
B^2	-0.013	1.16e+5	<0.0001
ABC	7.6e-6	0.073	0.7899
ABD	-1.2e-4	16.7	0.0004
ACD	2.2e-5	1.13	0.2988
BCD	2.2e-4	91.43	<0.0001
A^2B	-6.4e-4	169.7	<0.0001
A^2C	-4.5e-6	0.015	0.9022
A^2D	-4.1e-5	1.29	0.2672
AB^2	1.3e-4	8.00	0.0093
B^2C	-1.4e-4	13.26	0.0013
B^2D	-1.3e-3	1223.9	<0.0001
B^3	4.6e-3	2174.9	<0.0001

Table 12. The F-value, P-value and factor coefficients for Y_{II} expression in the LOP study.

Term	Coef.	F value	P value
Intercept	0.31	-	-
A	4.4e-3	4686.0	<0.0001
B	0.11	3.0e+5	<0.0001
C	-7.4e-4	110.5	<0.0001
D	1.7e-3	557.0	<0.0001
AB	4.1e-4	54.5	<0.0001
AC	-8.3e-7	4.2e-4	0.9839
AD	8.5e-6	0.044	0.8363
BC	1.3e-4	7.81	0.0101
BD	2.4e-3	2880.0	<0.0001
CD	-2.2e-4	42.3	<0.0001
A^2	1.1e-3	219.7	<0.0001
B^2	-0.022	88611.7	<0.0001
ABC	2.6e-5	0.22	0.6401
ABD	2.1e-6	1.5e-3	0.9694
ACD	-7.9e-6	0.038	0.8476
BCD	-1.9e-4	17.35	0.0003
A^2B	1.8e-4	3.65	0.0681
A^2C	-2.0e-6	7.9e-4	0.9777
A^2D	3.6e-6	2.7e-3	0.9590
AB^2	-7.3e-4	65.97	<0.0001
B^2C	3.6e-4	24.54	<0.0001
B^2D	8.5e-4	133.28	<0.0001
B^3	-1.1e-3	33.05	<0.0001

Table 13. Goodness-of-Fit indices for obtained Y_I and Y_{II} equations in the LOP study.

Indices	Y_I	Y_{II}
R^2	1.0000	1.0000
adjusted_ R^2	1.0000	1.0000
Pred_ R^2	0.9999	1.0000
Adeq. precision	846.66	1100.5

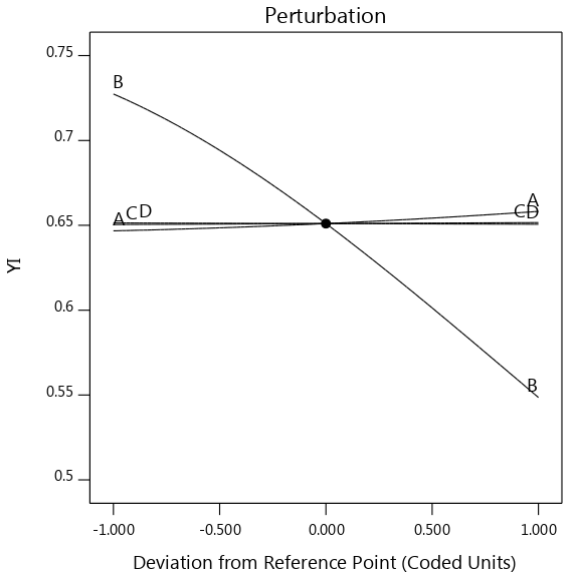

Fig. 3. Perturbation plot for parameters in Y_I.

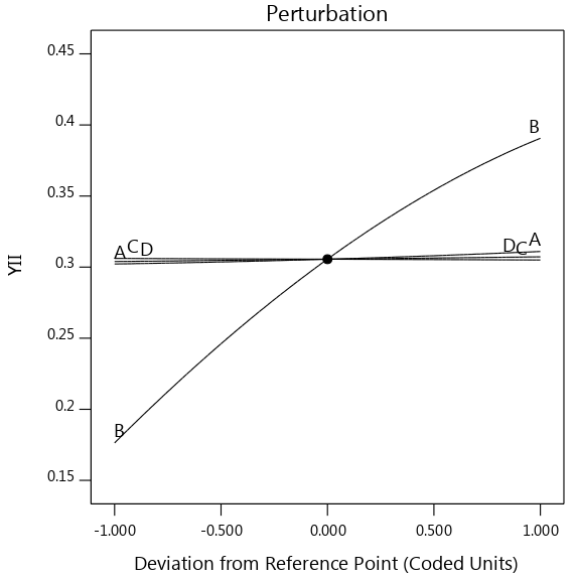

Fig. 4. Perturbation plot for parameters in Y_{II}.

As is shown the main factor effects C and D and their interactions with other factors could not be ignored and are included in the present model, however they aren't taken into account in the traditional design guidelines. Therefore, the present expressions are more accurate than what is applied traditionally.

Equations (8) and (9) are obtained from the cubic model after the removal of non-significant terms. Goodness of fit indices in Table 13 show the adequacy of the models.

$$Y_I = +0.700\text{-}0.032A+0.530B+0.023C\text{-}0.199D+0.061AB+0.964BD+2.998A^2\text{-}1.665B^2 \\ \text{-}3.253A^2B\text{-}1.152B^2D+0.869B^3 \tag{8}$$

$$Y_{II} = \text{-}0.182\text{-}0.224A+1.196B\text{-}0.022C+0.055D+0.816AB\text{-}0.407BD+0.922A^2\text{-}0.430B^2 \\ \text{-}0.711AB^2+0.737B^2D\text{-}0.208B^3 \quad (9)$$

Figures. 3 and 4 show the perturbation plot of all the factors, and Fig. 5 depicts the response surfaces for shape factors Y_I and Y_{II} based on simultaneous effects of the parameters. This figure besides the P-value, F-value and coefficient of cross-terms given in Tables 11 and 12 show noticeable interactions between factors A and B, together with factors B and D for both shape factors. Therefore, the predictive power of the model is demonstrated by adopting the factors interaction effects. The response surface is twisted by interaction effects which is the excellent feature of factorial design in discovering the interactions between factors [25]. From the Figs. 3-5, it is clear that both of the shape factors will be increased by increasing a_l/t ratio. Also, these figures indicate that Y_I decreases with the increase of w/t and h/t however Y_{II} increases with the increase of w/t and h/t. Meanwhile, these figures show that by increasing r/t, Y_{II} decreases, but Y_I increases.

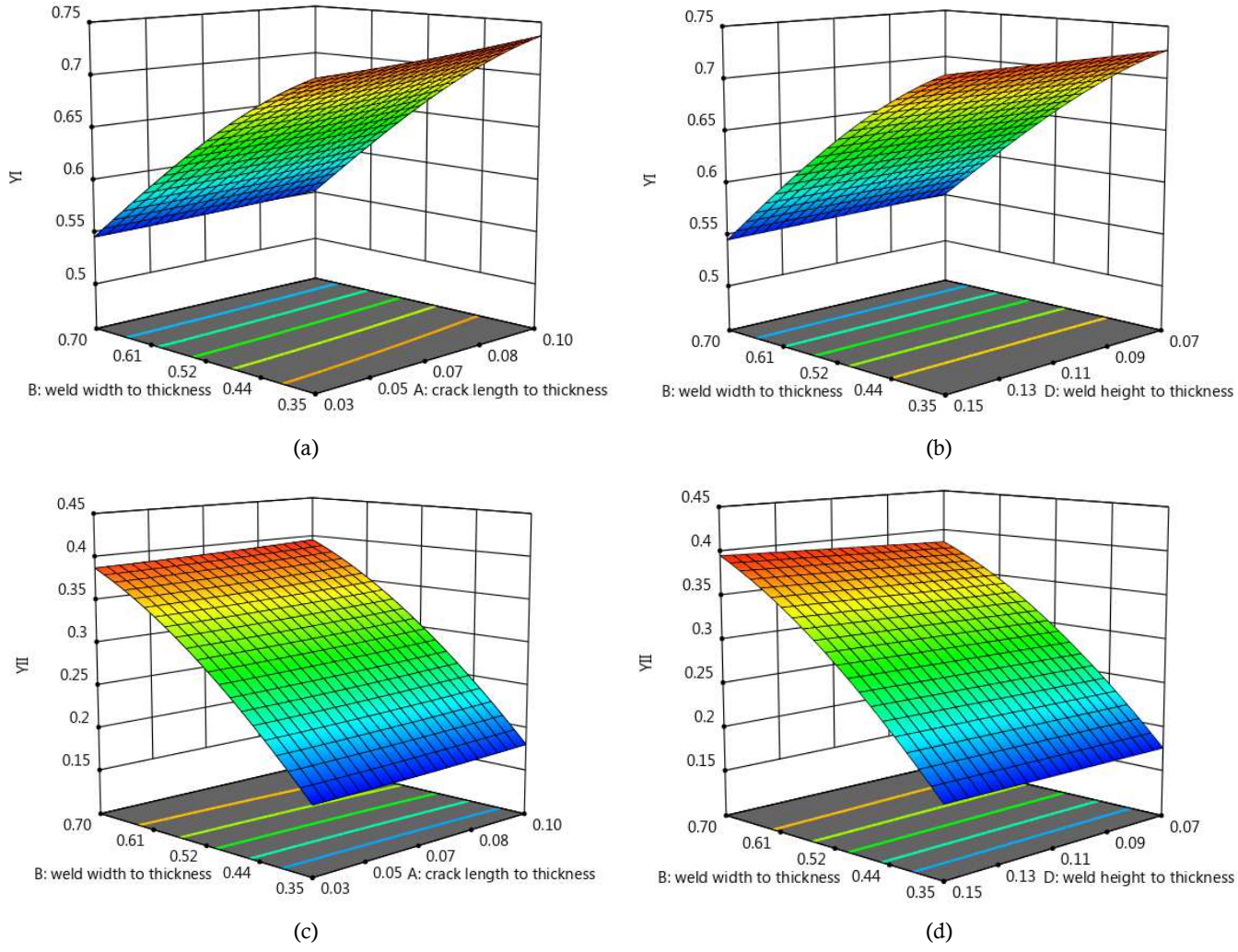

Fig. 5. Response surface for multiple effect of (a) w/t and a/t on Y_I, (b) h/t and w/t on Y_I, (c) w/t and a/t on Y_{II}, and (d) h/t and w/t on Y_{II} in the LOP study.

Figures 6 and 7 show values of shape factors Y_I and Y_{II} calculated by eqs. (8) and (9) compared with that from FEM analysis for h/t=0.075 and r/t=0.05, which are in good agreement. Hence, the obtained expressions for butt weld shape factors with inclined lack of penetration defect, can provide clear guidance for geometrical design of such joints.

3.3 The SIF expression for welded joint containing undercut defects

Table 14 shows the allowable undercut length for different levels of quality based on ISO5817 [16] and BS EN 25817 [17] standards. Acceptable ranges for the weld height based on these standards and for the groove angle (α) based on EN 29692 [18] standard were given in Tables 2 and 3, respectively. The r/t ratio in the present study is considered to range from 0 to 1. In order to provide an equation to cover the entire allowable ranges, undercut defect length, weld width, weld height, and toe radius were considered as given in Tables 15 and 19 in factorial design. The joint shown in Fig. 8 has a thickness (t) of 10 mm and w/t=0.7, h/t=0.15, r/t=0.1, and a_u/t=0.2. Based on the parameters' significance resulted in the screening experiment of 2-level factorial design, a number of levels are added for multi-level full factorial design.

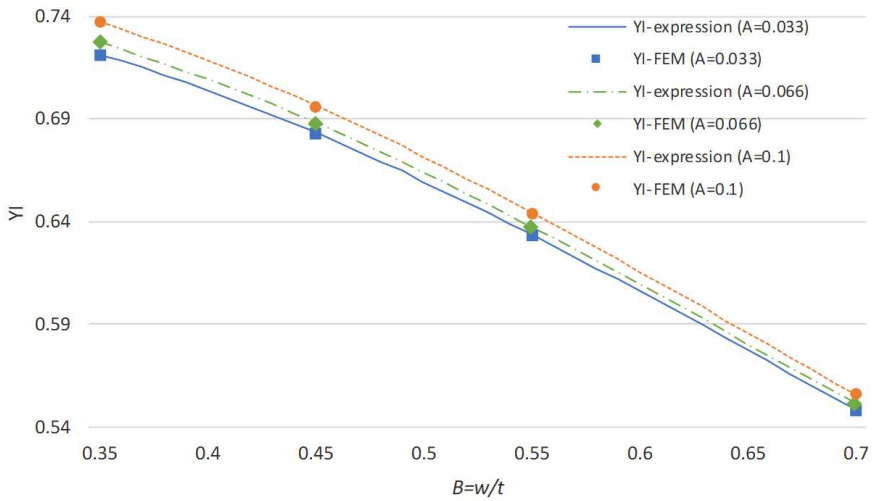

Fig. 6. Comparison of Y_I shape factor values calculated by expression eq. (8) and FEM analysis, h/t=0.075 and r/t=0.05.

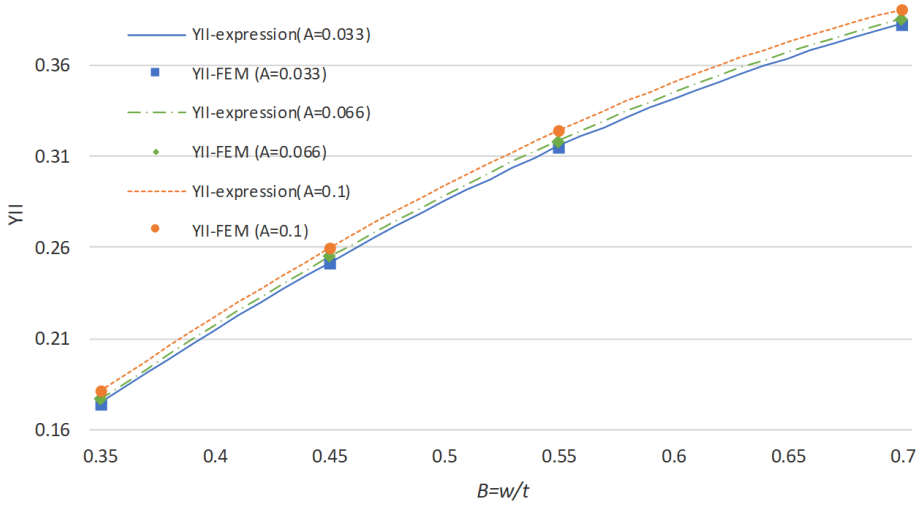

Fig. 7. Comparison of Y_{II} shape factor values calculated by expression eq. (9) and FEM analysis, h/t=0.075 and r/t=0.05.

Table 14. Acceptable ranges of the undercut length for standard quality levels.

Standard	Thickness (mm)	Limits for undercut for quality levels		
		D	C	B
ISO5817. [16]	0.5-3	a<0.2t	a<0.1t	Not permitted
	>3	a<0.2t (max 1 mm)	a<0.1t (max 0.5 mm)	a<0.05t (max 0.5 mm)
BS EN 25817. [17]	-	a<1.5 mm	a<1 mm	a<0.5 mm

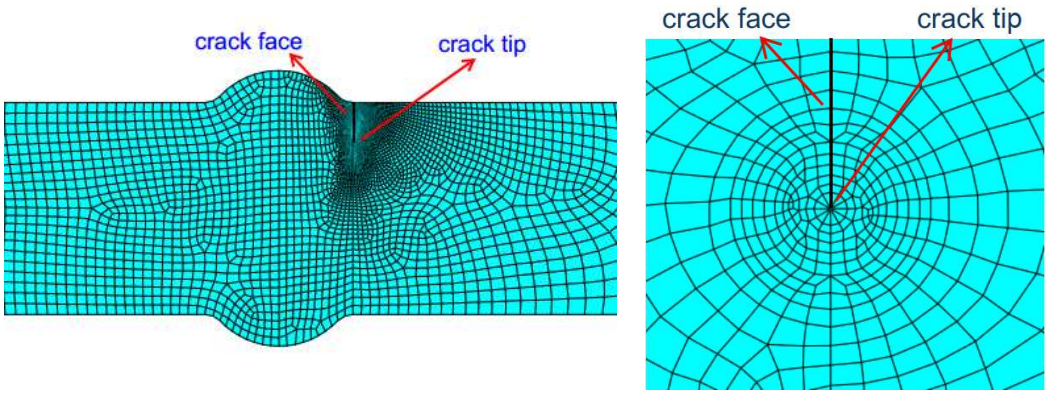

(a) (b)

Fig. 8. (1) FE model of butt welded joint with undercut and (2) FE model of meshes near the crack tip.

Table 15. Factor levels for the 2-level factorial design in the undercut study.

Factors	Low level (-1)	High level (+1)
$A=a_u/t$	0.1	0.2
$B=w/t$	0.35	0.7
$C=r/t$	0.05	0.1
$D=h/t$	0.075	0.15

Table 16. The 2-level factorial design Matrix and responses for undercut study.

Run	Factor Levels				Response
	A	*B*	*C*	*D*	Y_I
1	-1	-1	-1	1	1.2194
2	1	1	1	1	1.4105
3	1	-1	1	-1	1.3790
4	-1	-1	1	1	1.2170
5	-1	1	-1	-1	1.2790
6	-1	1	-1	1	1.3036
7	-1	-1	-1	-1	1.2202
8	1	-1	1	1	1.3789
9	1	1	-1	-1	1.4053
10	-1	1	1	1	1.2981
11	1	1	-1	1	1.4134
12	-1	1	1	-1	1.2770
13	1	-1	-1	-1	1.3799
14	1	1	1	-1	1.4041
15	1	-1	-1	1	1.3803
16	-1	-1	1	-1	1.2171

3.3.1 Two-level factorial experiments with undercut defects

As mentioned earlier, the shear stress at the crack tip of undercut defect is negligible under axial stress and hence, only, fracture mode I requires investigation. Lower and higher levels of the parameters given in Table 15 were used to obtain Y_I equation by RSM of 2-level factorial design. The design matrix and the responses of 2-level factorial design are shown in Table 16.

F-value, P-value and factor coefficients in Y_I expression in the case of 2-level factorial design are shown in Table 17. It is clear that a_u/t has the greatest significance and impact.

High values of goodness of fit indices, shown in Table 18, indicate the adequacy of the model as presented in eq. (10) bellow.

$$Y_I = 1.009+1.780A+0.154B-0.048C-0.542D-0.509AB+2.244AD+1.509BD-6.188ABD \tag{10}$$

Table 17. The F-value, P-value and coefficient of YI equation terms in the undercut study.

Term	Coef.	F value	P value
Intercept	1.32	-	-
A	0.070	1.6e+5	0.0016
B	0.025	20719.9	0.0044
C	-1.2e-3	18.3	0.0910
D	3.7e-3	163.3	0.0296
AB	-0.011	3703.7	0.0105
AC	4.3e-4	6.04	0.2460
AD	-1.9e-3	118.1	0.0584
BC	-2.3e-4	1.78	0.4099
BD	3.8e-3	483.0	0.0289
CD	-3.0e-4	3.08	0.3299
ABC	1.4e-5	6.7e-3	0.9479
ABD	2.0e-3	137.3	0.0542
ACD	3.8e-5	0.049	0.8619
BCD	-3.4e-4	3.79	0.3020

Table 18. Goodness-of-Fit Indices for obtained Y_I equation in the undercut study.

Indices	Value
R^2	0.9999
Adjusted_ R^2	0.9998
Pred_ R^2	0.9996
Adequate precision	251.60

3.3.2 Multi-level full factorial experiments with undercut defects

Referred to F-values of factors in Table 17 a number of levels are added for important parameters a_u/t and w/t in order to estimate the curvature in the response surface of shape factors. Parameter Levels for multi-level full factorial design in the case of undercut defect are shown in Table 19.
The design matrix and the responses are shown in Table 20 and the F-value, P-value and the factor coefficients of obtained expression are shown in Table 21.

Table 19. Factor levels for multi-level factorial design in undercut study.

Factors	Levels			
	1	2	3	4
$A=a_u/t$	0.05	0.1	0.15	0.2
$B=w/t$	0.35	0.525	0.7	
$C=r/t$	0.05	0.1		
$D=h/t$	0.075	0.15		

Table 20. A 2-level factorial design Matrix and responses for the undercut study.

Run	Factor Levels				Response	*Run*	Factor Levels				Response
	A	*B*	*C*	*D*	Y_I		*A*	*B*	*C*	*D*	Y_I
1	4	3	2	1	1.4041	25	3	2	2	2	1.3024
2	1	1	2	2	1.2268	26	2	2	1	1	1.2558
3	2	3	1	2	1.3036	27	4	3	1	1	1.4053
4	4	1	1	2	1.3803	28	3	2	2	1	1.3013
5	4	2	2	1	1.3913	29	1	2	2	1	1.2883
6	4	2	2	2	1.3919	30	2	1	2	1	1.2171
7	2	3	2	2	1.2981	31	4	2	1	1	1.3929
8	2	2	2	2	1.2567	32	3	3	1	2	1.3339
9	4	3	1	2	1.4134	33	1	2	1	2	1.3171
10	2	1	2	2	1.2170	34	1	3	2	2	1.3669
11	3	3	2	1	1.3191	35	2	1	1	1	1.2202
12	2	2	1	2	1.2617	36	3	1	2	1	1.2804
13	3	1	2	2	1.2804	37	1	2	1	1	1.2952
14	2	3	2	1	1.2769	38	4	1	2	2	1.3789
15	4	2	1	2	1.3943	39	1	1	1	1	1.2350
16	2	2	2	1	1.2530	40	3	3	2	2	1.3300
17	4	1	1	1	1.3799	41	1	2	2	2	1.3029
18	1	1	2	1	1.2268	42	4	3	2	2	1.4105
19	3	2	1	2	1.3059	43	2	1	1	2	1.2194
20	3	3	1	1	1.3206	44	3	2	1	1	1.3034
21	3	1	1	2	1.2823	45	4	1	2	1	1.3790
22	1	1	1	2	1.2339	46	1	3	2	1	1.3166
23	1	3	1	2	1.3823	47	1	3	1	1	1.3217
24	3	1	1	1	1.2823	48	2	3	1	1	1.2790

The resulting equation from the RSM is obtained after eliminating insignificant terms from the cubic model and is given in eq. (11).

$$Y_I = 1.166\text{-}2.303A+0.712B\text{-}0.086C\text{-}0.689D\text{-}5.401AB\text{-}0.034AD+2.441BD+28.895A^2 \\ \text{-}0.465B^2\text{-}12.027ABD+8.422A^2B+18.006A^2D+2.856AB^2\text{-}60.146A^3 \tag{11}$$

The high values of all model adequacy indices indicated in Table 22 show that the model has a very good accuracy and adequacy.
Perturbation plot in Fig. 9 shows that the a_u/t ratio (factor A) is the most effective parameter on the response. The increasing of this ratio initially causes to a decrease in Y_I and then makes it increase after a minimum point. That's because as crack grows, it goes away from the stress concentration area in weld toe caused by reinforcement and as a result, shape factor decreases. After a specific length, crack length's impact on shape factor becomes predominant and its growth causes an increase in the shape factor. Y_I increases with increasing of both w/t (factor B) and h/t (factor D) parameters. Y_I reduces with the increase of r/t ratio (factor C). The 3D plots of simultaneous factor effects are shown in Fig. 10. These plots and ANOVA results show that there are significant interactions between A and B, A and D, and B and D factors. Both perturbation and Tables 17 and 21 show that Y_I decreases with the increasing of r/t ratio. This means that the existence of smooth transition at the weld toe is appropriate to extend the life of butt joints containing the undercut defects.

Table 21. The F-value, P-value and the factors coefficients in Y_I expression for undercut defect.

Term	Coef.	F value	P value
Intercept	1.27	-	-
A	0.071	1121.1	<0.0001
B	0.028	1183.3	<0.0001
C	-1.6e-3	3.24	0.0845
D	1.1e-3	1.61	0.2165
AB	-0.022	1010.1	<0.0001
AC	1.8e-3	10.9	0.0030
AD	-5.2e-3	87.2	<0.0001
BC	-3.3e-4	0.41	0.5261
BD	6.2e-3	146.9	<0.0001
CD	-5.8e-4	1.96	0.1742
A^2	0.072	5946.9	<0.0001
B^2	-3.3e-3	14.3	0.0009
ABC	2.0e-4	0.090	0.7663
ABD	-5.9e-3	75.51	<0.0001
ACD	5.2e-4	0.88	0.3576
BCD	-6.0e-4	1.39	0.2499
A^2B	8.3e-3	52.67	<0.0001
A^2C	-1.5e-3	2.48	0.1286
A^2D	3.8e-3	16.58	0.0004
AB^2	6.6e-3	30.91	<0.0001
B^2C	4.0e-4	0.21	0.6524
B^2D	2.8e-3	10.31	0.0037
A^3	2.1e-3	148.0	<0.0001

Table 22. Goodness-of-Fit Indices for obtained Y_I equation in the undercut study.

Indices	Value
R^2	0.9975
Adjusted_ R^2	0.9964
Pred_ R^2	0.9942
Adequate precision	99.296

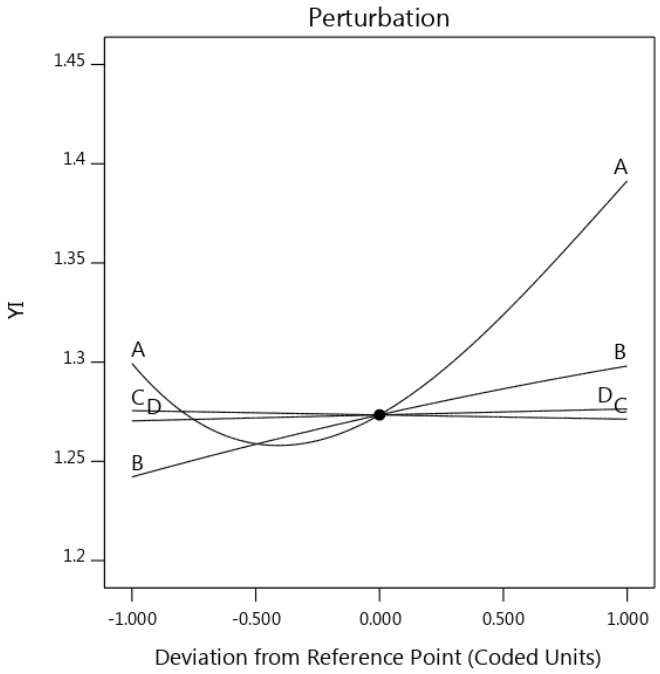

Fig. 9. Perturbation plot for parameters in Y_I.

Figure 11 shows shape factor Y_I calculated by eq. (11) compared with that from FEM analysis result where h/t=0.075 and r/t=0.05. The results indicate that shape factor calculated by eq. (11) and the FEM analysis are in good agreement. Hence, the obtained expression for shape factor of welded butt joint with undercut defect, can provide clear guidance for geometrical design of such joints.

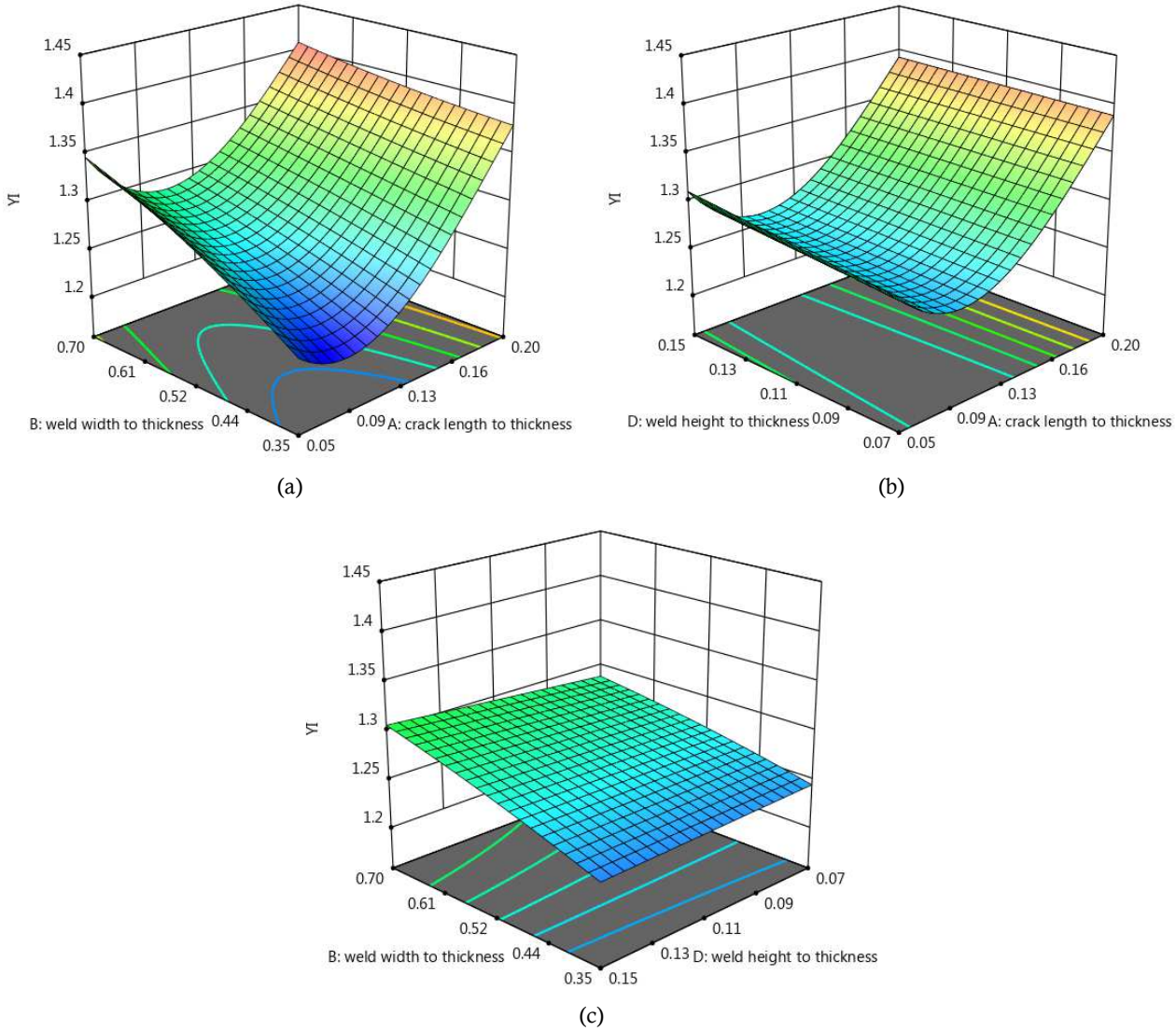

Fig. 10. Response surface for multiple effect of (a) w/t and a/t (b) h/t and a/t and (c) h/t and w/t in the undercut study.

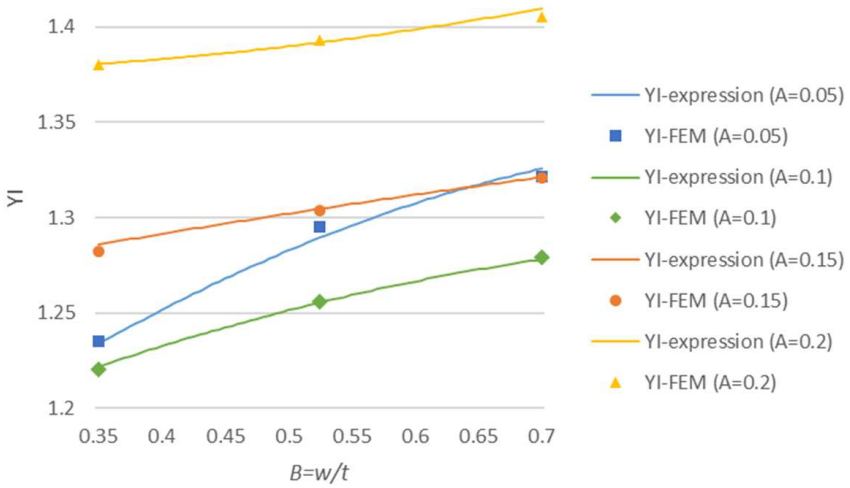

Fig. 11. Comparison of shape factor Y_I yielded by eq. (11) and FEM analysis, h/t=0.075 and r/t=0.05.

4. Conclusions

Shape Factors as a key parameter in fracture mechanics are of paramount importance in designing welded joints which naturally contain crack like defects. Using "Response Surface Method" in the present research, some expressions

for inclined LOP and undercut shape factors of butt welded joints were obtained as a function of four independent and dimensionless geometric parameters namely, the ratios of width, height and toe radius of the weld, and crack length to the thickness of the base metal for the sake of generality. It was found that shape factor Y_I of butt joint containing inclined LOP increases with increase in crack length or weld toe transition radius but decreases as weld width or weld height increases. However, shape factor Y_{II} of butt welded joint containing inclined LOP increases with the increase of crack length, weld width or weld height but decreases as toe transition radius increases. In both of shape factors, weld width has the greatest effect, and the effects of weld toe transition radius and weld height are not as important. In the case of butt welded joints containing undercut defect, the stress intensity factor increases with the increase in crack length, weld height or weld width, and in particular the crack length, but decreases when toe transition radius increases. The values of F-and P statistics in ANOVA and response surfaces of shape factors Y_I and Y_{II} show that the interaction effects between height and width of weld and crack length are very high. It is made obvious that the predictive power of the obtained model is indebted to coverage of factors interaction effects that made possible by factorial design. Design of Butt welded joints could be performed based on the stress intensity factor expressions given in this paper. In addition, critical crack length, critical stresses, and life or reliability of butt welded joints with unavoidable inclined LOP and undercut defects can also be predicted in the light of developed expressions with sufficient accuracy and ease of application.

Conflict of Interest

The authors declared no potential conflicts of interest with respect to the research, authorship and publication of this article.

Funding

The authors received no financial support for the research, authorship and publication of this article.

References

[1] Nguyen, T.N., and Wahab, M.A., The effect of weld geometry and residual stresses on the fatigue of welded joints under combined loading, *Journal of Materials Processing Technology*, 77(1), 1998, 201-208.
[2] Al-Mukhtar, A., Biermann, H., Henkel, S., and Hübner, P., Comparison of the stress intensity factor of load-carrying cruciform welded joints with different geometries, *Journal of Materials Engineering and Performance*, 19(6), 2010, 802-809.
[3] Burgess, N., *Quality assurance of welded construction*, CRC Press, 1989.
[4] Ali, A., and Sanuddin, A., Characterization of ASTM A516 Grade 70 Fusion Welded Joints, *International Review of Mechanical Engineering*, 3(5), 2009, 531-542.
[5] Handbook, A., *Properties and selection: irons, steels, and high-performance alloys, Vol. 1, ASM International*, 1990.
[6] Hu, L., Huang, J., Li, Z., and Wu, Y., Effects of preheating temperature on cold cracks, microstructures and properties of high power laser hybrid welded 10Ni3CrMoV steel, *Materials & Design*, 32(4), 2011, 1931-1939.
[7] Liu, Y., and Chan, S., Modern design method using NIDA for scaffolding systems, *Tubular Structures XIII. Hong Kong: CRS Press*, 2010, 443-447.
[8] Rahman, S., Probabilistic fracture mechanics: J-estimation and finite element methods, *Engineering Fracture Mechanics*, 68(1), 2001, 107-125.
[9] Wang, T., Yang, J., Liu, X., Dong, Z., and Fang, H., Stress intensity factor expression for butt joint with single-edge crack considering the effect of joint shape, *Materials & Design*, 36, 2012, 748-756.
[10] Melchers, R.E., and Beck, A.T., *Structural reliability analysis and prediction*, John Wiley & Sons, 2018.
[11] Lee, M., Strength, stress and fracture analyses of offshore tubular joints using finite elements, *Journal of Constructional Steel Research*, 51(3), 1999, 265-286.
[12] Hobbacher, A., Stress intensity factors of welded joints*, Engineering fracture mechanics*, 46(2), 1993, 173-182.
[13] Frank, K.H., and Fisher, J.W., Fatigue strength of fillet welded cruciform joints, *Journal of the Structural Division*, 105(9), 1979, 1727-1740.
[14] Hobbacher, A., *Recommendations for fatigue design of welded joints and components*, Springer, 2009.
[15] Wang, T., Yang, J., Liu, X., Dong, Z., and Fang, H., Stress intensity factor expression for center-cracked butt joint considering the effect of joint shape, *Materials & Design*, 35, 2012, 72-79.
[16] DIN, E., *5817: Welding–fusion-welded joints in steel, nickel, titanium and their alloys (beam welding excluded)–quality levels for imperfections*, 2006.
[17] 25817, T.E.S.E., *Arc-welded joints in steel - Guidance on quality levels for imperfections*, 1992.
[18] Standard, B, *Specification for "Metal-arc welding with covered electrode, gas-shielded metal-arc welding and gas welding-Joint preparations for steel*, BS EN 29692, 1994.
[19] Wu, X.-F., Dzenis, Y.A., and Gokdag, E., Edge-cracked orthotropic bimaterial butt joint under antiplane singularity, *International Journal of Nonlinear Sciences and Numerical Simulation*, 5(4), 2004, 347-354.
[20] Reedy, E., and Guess, T., Butt joint tensile strength: interface corner stress intensity factor prediction, *Journal of Adhesion Science and Technology*, 9(2), 1995, 237-251.

[21] Kirkhope, K., Bell, R., Caron, L., Basu, R., and Ma, K.-T., Weld detail fatigue life improvement techniques. Part 1, *Marine Structures*, 12(6), 1999, 447-474.
[22] Kirkhope, K., Bell, R., Caron, L., Basu, R., and Ma, K.-T., Weld detail fatigue life improvement techniques. Part 2: application to ship structures, *Marine Structures*, 12(7-8), 1999, 477-496.
[23] Ninh, N.T., and Wahab, M.A., The effect of residual stresses and weld geometry on the improvement of fatigue life, *Journal of Materials Processing Technology*, 48(1-4), 1995, 581-588.
[24] Broek, D., *Elementary engineering fracture mechanics*, Springer Science & Business Media, 2012.
[25] Montgomery, D.C., and Runger, G.C., *Applied statistics and probability for engineers, (With CD)*, John Wiley & Sons, 2007.
[26] Guinea, G.V., Planas, J., and Elices, M., KI evaluation by the displacement extrapolation technique, *Engineering Fracture Mechanics*, 66(3), 2000, 243-255.
[27] Courtin, S., Gardin, C., Bezine, G., and Hamouda, H.B.H., Advantages of the J-integral approach for calculating stress intensity factors when using the commercial finite element software ABAQUS, *Engineering Fracture Mechanics*, 72(14), 2005, 2174-2185.
[28] Zhu, W., and Smith, D., On the use of displacement extrapolation to obtain crack tip singular stresses and stress intensity factors, *Engineering Fracture Mechanics*, 51(3), 1995, 391-400.
[29] Banks-Sills, L., and Einav, O., On singular, nine-noded, distorted, isoparametric elements in linear elastic fracture mechanics, *Computers & Structures*, 25(3), 1987, 445-449.
[30] Thoft-Cristensen, P., and Baker, M.J., *Structural reliability theory and its applications*, Springer Science & Business Media, 2012.

ORCID iD

Akbar Jafari https://orcid.org/0000-0002-4167-1746
Mohsen Rezaeian Akbarzadeh https://orcid.org/0000-0001-7738-2201